PERGAMON

International Journal of Solids and Structures 36 (1999) 1081–1098

INTERNATIONAL JOURNAL OF SOLIDS and STRUCTURES

On a higher order analysis of laminated composite strips with extension-twist coupling

Andrew Makeev*, Erian Armanios

School of Aerospace Engineering, Georgia Institute of Technology, Atlanta, GA 30332-0150, U.S.A.

Received 20 March 1997

Abstract

A finite displacement analysis for extension-twist coupling in pretwisted laminated composite strips is presented. A new formulation of the kinematics is constructed by neglecting the terms of order of the square of the maximum strain magnitude in the strain–displacement relations. The closed-form extension-twist relationships are derived and the influence of out-of-plane shear strains on the results is estimated. The accuracy of the model is assessed through comparison with test data and analytical predictions.

1. Introduction

Elastic tailoring of composites allows a unique flexibility to meet the design requirements efficiently and economically. Coupling of deformation modes such as extension-twist and bending-twist can be created in composite structures by an appropriate selection of material, geometry, and stacking sequence. In order to implement elastic tailoring in practical applications, an accurate prediction of their response under loading is required.

Extension-twist coupling in laminated composite strips can be created by using antisymmetric stacking sequences. Such laminates will twist when subjected to axial load. Test data for thin strip laminates with such stacking sequences show a nonlinear axial force-twist dependence. This is due to the low torsional to extensional stiffness ratio and cannot be predicted using the small displacement theories. In order to explain this nonlinear behavior, a finite displacement model was developed by Armanios et al. (1996). The closed-form solution developed in this model was in good agreement with other analytical results and test data. In developing the model, the terms in the strain–displacement relations were classified by the order of their maximum magnitude. The maximum magnitude of strain was denoted by ε. First, the terms of order ε were neglected

* Corresponding author.

0020–7683/99/$ - see front matter
PII: S0020–7683(97)00338–7

compared to unity. Second, the terms of order $\varepsilon^{3/2}$ and higher were neglected. In order to provide a consistent analysis, it is important to investigate the influence of the higher order terms in the strain–displacement relations on the results. This work presents a closed-form solution for the extension-twist behavior of pretwisted thin laminated strips neglecting the terms of $O(\varepsilon^2)$ and higher in the strain–displacement relationships, and assesses the accuracy of the previous model.

2. Analysis

Consider a laminated strip shown in Fig. 1. The thickness h of the laminate is small relative to the width $2b$ which is small compared to the length L. That is

$$h \ll 2b \ll L \tag{1}$$

The strip has a pretwist about the longitudinal axis X. Assume that the strains are small (negligible compared to one) and independent of the longitudinal direction; the pretwist rate θ_0 and the elastic twist rate θ are constant; and the material is linearly elastic.

The middle surface of the strip is referred to the material coordinates x and y, while the transverse material coordinate is denoted by z. If the strip is flat, the position vector of an arbitrary point is defined as

$$\mathbf{r}_f = x\hat{\mathbf{i}} + y\hat{\mathbf{j}} + z\hat{\mathbf{k}}, \qquad 0 \leqslant x \leqslant L, \quad -b \leqslant y \leqslant b, \quad -\frac{h}{2} \leqslant z \leqslant \frac{h}{2} \tag{2}$$

where $\hat{\mathbf{i}}$, $\hat{\mathbf{j}}$, $\hat{\mathbf{k}}$ are the unit base vectors of the reference Cartesian coordinate system XYZ. The

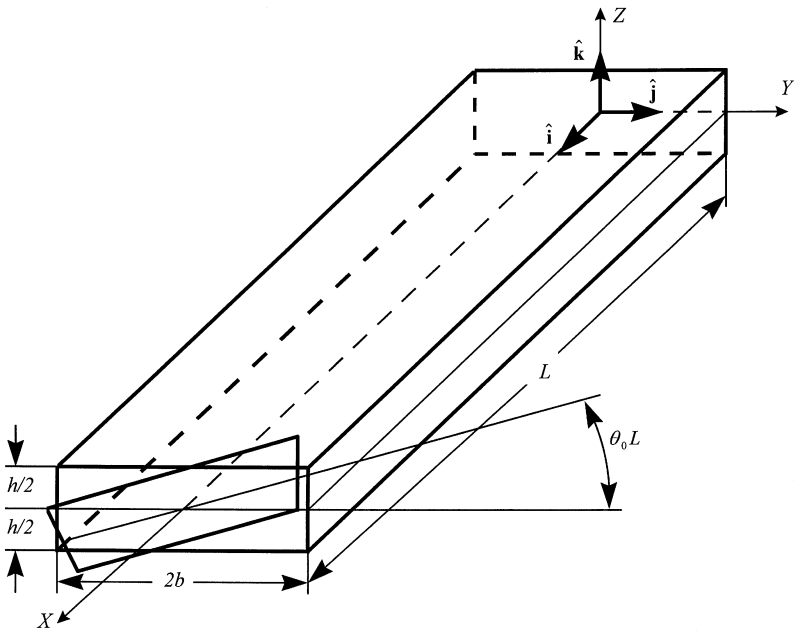

Fig. 1. Laminate geometry.

position vector $\mathbf{r}_0$ of a material point in the initial state is derived as follows. First, a rigid cross-section is rotated about the X-axis. Second, the out-of-plane strains caused by the previous step are set to zero by rotating straight line elements perpendicular to the middle surface. The result is

$$\mathbf{r}_0 = \left(x - \frac{\theta_0 yz}{\sqrt{1+(\theta_0 y)^2}}\right)\hat{\mathbf{i}} - y\hat{\mathbf{e}}_{20} + \frac{z}{\sqrt{1+(\theta_0 y)^2}}\hat{\mathbf{e}}_{30} \tag{3}$$

where

$$\begin{aligned}\hat{\mathbf{e}}_{20} &= \cos\theta_0 x\hat{\mathbf{j}} + \sin\theta_0 x\hat{\mathbf{k}}\\ \hat{\mathbf{e}}_{30} &= -\sin\theta_0 x\hat{\mathbf{j}} + \cos\theta_0 x\hat{\mathbf{k}}\end{aligned} \tag{4}$$

The position vector $\mathbf{r}$ of the material point in the deformed state is derived the same way as in the initial state. However, a small displacement field is added to account for all strain components

$$\mathbf{r} = \left(x - \frac{(\theta_0+\theta)yz}{\sqrt{1+(\theta_0+\theta)^2 y^2}} + u\right)\hat{\mathbf{i}} + (y+v)\hat{\mathbf{e}}_2 + \left(\frac{z}{\sqrt{1+(\theta_0+\theta)^2 y^2}} + w\right)\hat{\mathbf{e}}_3 \tag{5}$$

where

$$\begin{aligned}\hat{\mathbf{e}}_2 &= \cos(\theta_0+\theta)x\hat{\mathbf{j}} + \sin(\theta_0+\theta)x\hat{\mathbf{k}}\\ \hat{\mathbf{e}}_3 &= -\sin(\theta+\theta_0)x\hat{\mathbf{j}} + \cos(\theta_0+\theta)x\hat{\mathbf{k}}\end{aligned} \tag{6}$$

and

$$u = \varepsilon_0 x + U(y,z), \quad v = V(y,z), \quad w = W(y,z) \tag{7}$$

are the components of the small displacement vector.

The Lagrangian strain tensor components are defined as

$$2\varepsilon_{ij} = g_{ij} - h_{ij} \tag{8}$$

where g_{ij} and h_{ij} are the metric tensor components in the deformed and the initial states, respectively

$$\begin{aligned}g_{ij} &= \frac{\partial \mathbf{r}}{\partial x^i}\cdot\frac{\partial \mathbf{r}}{\partial x^j}\\ h_{ij} &= \frac{\partial \mathbf{r}_0}{\partial x^i}\cdot\frac{\partial \mathbf{r}_0}{\partial x^j}\end{aligned} \tag{9}$$

The following limits are imposed on the maximum values of the kinematic parameters

$$\begin{aligned}&\theta_0 h, \quad \theta h = O(\varepsilon)\\ &(\theta_0 b)^2, \quad (\theta b)^2 = O(\varepsilon)\\ &\frac{\partial U}{\partial y}, \quad \frac{\partial U}{\partial z}, \quad \frac{\partial V}{\partial y}, \quad \frac{\partial V}{\partial z}, \quad \frac{\partial W}{\partial y}, \quad \frac{\partial W}{\partial z} = O(\varepsilon)\\ &\theta_0 V, \quad \theta_0 W, \quad \theta V, \quad \theta W = O(\varepsilon^{3/2})\end{aligned} \tag{10}$$

where ε denotes the maximum magnitude of strain. The terms of $O(\varepsilon^2)$ and higher will be neglected in the strain–displacement relations.

According to eqns (3)–(10), the out-of-plane engineering strains can be expressed as

$$\begin{aligned}
\varepsilon_{zz} &= W_{,z} - (\theta_0 + \theta) y U_{,z} \\
\gamma_{yz} &= W_{,y} + V_{,z} - (\theta_0 + \theta) y U_{,y} \\
\gamma_{xz} &= U_{,z} + (\theta_0 + \theta)(-y\varepsilon_0 + y W_{,z} + V - z V_{,z})
\end{aligned} \tag{11}$$

where the partial derivatives are denoted by commas.

Since the strip is thin, the out-of-plane shear strains are replaced by their average values with respect to thickness

$$\gamma_{yz} = \gamma_{yz}(y), \quad \gamma_{xz} = \gamma_{xz}(y) \tag{12}$$

Moreover, nondeformability in the z-material direction is assumed, i.e.

$$\varepsilon_{zz} = 0 \tag{13}$$

Substitute eqns (12) and (13) into eqns (11), integrate the resulting expressions, and neglect the terms of $O(\varepsilon^2)$ to obtain the following linear in z form of the small displacement field

$$\begin{aligned}
U &= U_0(y) - z U_1(y) \\
V &= V_0(y) - z V_1(y) \\
W &= W_0(y) - z(\theta_0 + \theta) y U_1(y)
\end{aligned} \tag{14}$$

According to eqns (3)–(9), and (14), the engineering strain–displacement relationships take the form

$$\begin{aligned}
&\varepsilon_{ij} = \varepsilon^0_{ij} - z k_{ij}, \quad (i,j = x,y,z) \\
&\varepsilon^0_{xx} = \varepsilon_0 + \tfrac{1}{2}(\theta^2 + 2\theta_0\theta) y^2, \quad \kappa_{xx} = 0 \\
&\varepsilon^0_{yy} = V_{0,y}, \quad \kappa_{yy} = V_{1,y} \\
&\varepsilon_{zz} = 0 \\
&\gamma_{yz} = -V_1 + W_{0,y} - (\theta_0 + \theta) y U_{0,y} \\
&\gamma_{xz} = -U_1 + (\theta_0 + \theta)(V_0 - \varepsilon_0 y) \\
&\gamma^0_{xy} = U_{0,y} + (\theta_0 + \theta)(y W_{0,y} - W_0), \quad \kappa_{xy} = U_{1,y} + 2\theta
\end{aligned} \tag{15}$$

The equilibrium equations and boundary conditions for a cantilever strip subjected to an axial force F and a torque T can be derived using the principle of virtual work

$$\int_{-b}^{b} \mathrm{d}y \int_{-(h/2)}^{h/2} \sigma^{ij} \delta\varepsilon_{ij} \sqrt{g}\, \mathrm{d}z - T\delta\theta - F\delta\varepsilon_0 = 0 \tag{16}$$

where σ^{ij} are the second Piola–Kirchhoff stress tensor components. Summation over the repeated indices is assumed. The Jacobian

$$\sqrt{g} = \frac{\partial \mathbf{r}_0}{\partial x} \cdot \left(\frac{\partial \mathbf{r}_0}{\partial y} \times \frac{\partial \mathbf{r}_0}{\partial z} \right) = 1 \tag{17}$$

if the terms of $O(\varepsilon)$ are neglected compared to unity. Denote the forces and moments per unit length of the middle surface by

$$(N_{xx}, N_{yy}, Q_y, Q_x, N_{xy}, M_{xx}, M_{yy}, M_{xy}) = \int_{-(h/2)}^{h/2} (\sigma^{xx}, \sigma^{yy}, \sigma^{yz}, \sigma^{xz}, \sigma^{xy}, z\sigma^{xx}, z\sigma^{yy}, z\sigma^{xy})\, \mathrm{d}z \tag{18}$$

where the subscripts do not denote covariant tensor components.

The lateral surfaces of the strip are traction free. Therefore, at $y = \pm b$

$$N_{yy} = N_{xy} = Q_y = M_{yy} = M_{xy} = 0 \tag{19}$$

Substitute eqns (15), (17)–(19) into eqn (16), and reduce the resulting equilibrium equations and boundary conditions to

$$N_{xy} = Q_y = M_{yy} = 0 \tag{20}$$

$$N_{yy} = (\theta_0 + \theta) M_{xy} \tag{21}$$

$$M_{xy,y} - Q_x = 0 \tag{22}$$

$$\int_{-b}^{b} [N_{xx}(\theta_0 + \theta) y^2 - 2M_{xy}]\, \mathrm{d}y = T \tag{23}$$

$$\int_{-b}^{b} [N_{xx} + (\theta_0 + \theta) M_{xy}]\, \mathrm{d}y = F \tag{24}$$

where ε_0 and $V_{0,y} = \varepsilon^0_{yy}$ were neglected compared to one in deriving eqn (23). According to eqn (23), eqn (24) can be written in the following form

$$\begin{aligned} F &= \int_{-b}^{b} \left[N_{xx} + (\theta_0 + \theta) M_{xy} + \frac{(\theta_0 + \theta)^2 y^2}{2} N_{xx} - \frac{(\theta_0 + \theta)^2 y^2}{2} N_{xx} \right] \mathrm{d}y \\ &= \int_{-b}^{b} N_{xx} \left[1 + \frac{(\theta_0 + \theta)^2 y^2}{2} \right] \mathrm{d}y - \frac{(\theta_0 + \theta)}{2} T \end{aligned} \tag{25}$$

Neglect $[(\theta_0 + \theta)^2 y^2]/2$ compared to one to obtain

$$\int_{-b}^{b} N_{xx}\, \mathrm{d}y = F + \frac{(\theta_0 + \theta)}{2} T \tag{26}$$

It is worth noting that if the applied torque T is equal to zero, the boundary conditions (23) and (26) can be derived by neglecting the terms of $O(\varepsilon^{3/2})$ in the strain–displacement relations (15).

Assume that the constitutive relations are given in local rectangular Cartesian coordinates. Although the base vectors

$$\frac{\partial \mathbf{r}_0}{\partial x}, \quad \frac{\partial \mathbf{r}_0}{\partial y}, \quad \frac{\partial \mathbf{r}_0}{\partial z} \tag{27}$$

of the material coordinate system (x, y, z) in the initial state are not orthogonal, transformation to the orthogonal coordinates would introduce correction of $O(\varepsilon^2)$ in the strain field as shown in Armanios et al. (1996).

Equation (13) implies that for each lamina

$$E_{33} \to \infty, \quad \nu_{13} = \nu_{23} = 0 \tag{28}$$

where E_{33}, ν_{13} and ν_{23} are Young's modulus and Poisson's ratios associated with the transverse material direction. Indices 1, 2, 3 denote the principal material axes. Therefore, the in-plane components of the lamina stiffness matrix are the same as those for the plane stress state.

The constitutive relations for an antisymmetric laminate can be written in the following form

$$\begin{Bmatrix} N_{xx} \\ N_{yy} \\ M_{xy} \end{Bmatrix} = \begin{bmatrix} A_{11} & A_{12} & B_{16} \\ A_{12} & A_{22} & B_{26} \\ B_{16} & B_{26} & D_{66} \end{bmatrix} \begin{Bmatrix} \varepsilon^0_{xx} \\ \varepsilon^0_{yy} \\ -\kappa_{xy} \end{Bmatrix} \tag{29a}$$

$$\begin{Bmatrix} N_{xy} \\ M_{xx} \\ M_{yy} \end{Bmatrix} = \begin{bmatrix} A_{66} & B_{16} & B_{26} \\ B_{16} & D_{11} & D_{12} \\ B_{26} & D_{12} & D_{22} \end{bmatrix} \begin{Bmatrix} \gamma^0_{xy} \\ -\kappa_{xx} \\ -\kappa_{yy} \end{Bmatrix}$$

$$Q_y = A_{44}\gamma_{yz}, \quad Q_x = A_{55}\gamma_{xz} \tag{29b}$$

The stiffness parameters are defined as

$$(A_{ij}, B_{ij}, D_{ij}) = \int_{-(h/2)}^{h/2} \bar{Q}_{ij}(1, z, z^2)\, \mathrm{d}z \tag{30}$$

where $\bar{Q}_{ij}$ are the components of the lamina stiffness matrix in the (x, y, z)-coordinates (Vinson and Sierakowski, 1986).

The axial force N_{xx} and the twisting moment M_{xy} per unit length of the middle surface will be expressed in terms of the axial strain and the twist rate. The resulting equations will be substituted into the boundary conditions (23) and (26) to get the extension-twist relationships. It is worth noting that the quantities

$$\frac{B_{16}}{A_{12}}(\theta_0+\theta), \quad \frac{B_{26}}{A_{22}}(\theta_0+\theta), \quad \frac{\alpha_{12}}{\beta}(\theta_0+\theta), \quad \frac{\alpha_{12}}{\alpha_{11}}(\theta_0+\theta), \quad \sqrt{\frac{\alpha_{22}}{\beta}}(\theta_0+\theta), \quad \sqrt{\frac{D_{66}}{A_{12}}}(\theta_0+\theta) \tag{31}$$

where α_{ij} and β are defined by

$$\alpha_{11} = A_{11} - \frac{A_{12}^2}{A_{22}}, \quad \alpha_{12} = B_{16} - \frac{A_{12}B_{26}}{A_{22}}$$

$$\alpha_{22} = D_{66} - \frac{B_{26}^2}{A_{22}}$$

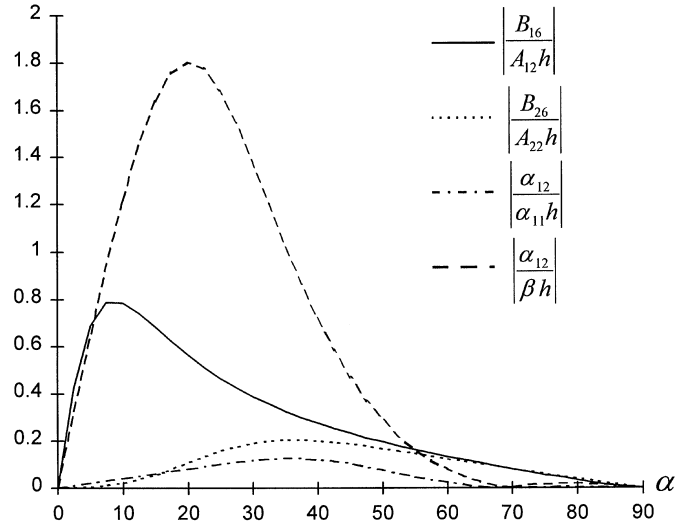

Fig. 2. Estimation of parameters.

$$\beta = A_{55} \tag{32}$$

can be neglected compared to one for a practical material system. A numerical verification of this observation is provided in Figs 2 and 3 where the absolute values of

$$\frac{B_{16}}{A_{12}h}, \quad \frac{B_{26}}{A_{22}h}, \quad \frac{\alpha_{12}}{\beta h}, \quad \frac{\alpha_{12}}{\alpha_{11}h}, \quad \sqrt{\frac{\alpha_{22}}{\beta}}\frac{1}{h}, \quad \text{and} \quad \sqrt{\frac{D_{66}}{A_{12}}}\frac{1}{h}$$

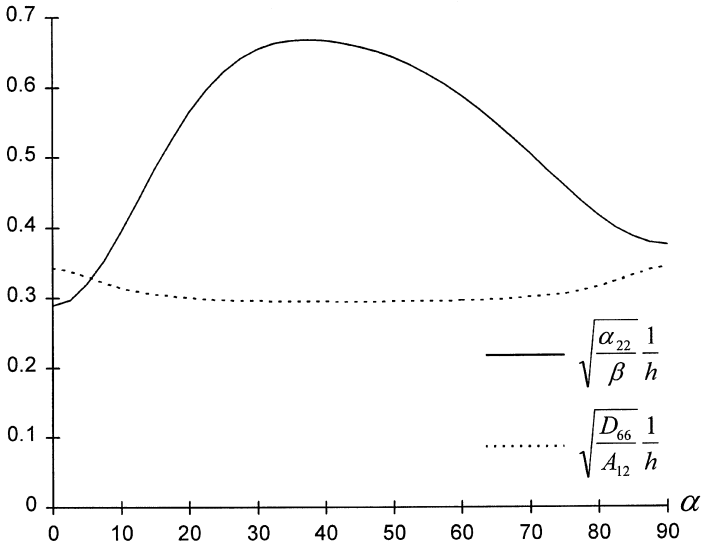

Fig. 3. Estimation of parameters.

Table 1
Properties of T300/954-3 Graphite/ Cyanate material system

$E_{11} = 135.6$ GPa
$E_{22} = 9.9$ GPa
$G_{12} = G_{13} = 4.2$ GPa
$G_{23} = 2.5$ GPa
$v_{12} = 0.3$

are plotted vs the ply angle α for angle ply laminates $[\alpha_n/-\alpha_n]_T$. The laminates are made of ICI Fiberite T300/954-3 Graphite/Cyanate material system with properties given in Table 1. The absolute values of the variables in Figs 2 and 3 are of $O(1)$. When multiplied by $(\theta_0+\theta)h$, as in (31), those quantities will be of $O(\varepsilon)$ according to eqns (10).

Substitute for N_{yy} and M_{xy} from eqn (29a) into eqn (21) to obtain

$$\varepsilon^0_{yy} = -\left[\frac{A_{12}-(\theta_0+\theta)B_{16}}{A_{22}-(\theta_0+\theta)B_{26}}\right]\varepsilon^0_{xx} - \left[\frac{B_{26}-(\theta_0+\theta)D_{66}}{A_{22}-(\theta_0+\theta)B_{26}}\right](-\kappa_{xy}) \tag{33}$$

Neglect

$$\frac{(\theta_0+\theta)B_{16}}{A_{12}}, \quad \frac{(\theta_0+\theta)B_{26}}{A_{22}} \tag{34}$$

as terms of $O(\varepsilon)$ compared to one, and rewrite eqn (33) as follows

$$\varepsilon^0_{yy} = -\frac{A_{12}}{A_{22}}\left[\varepsilon^0_{xx} + \frac{(\theta_0+\theta)D_{66}\kappa_{xy}}{A_{12}}\right] - \frac{B_{26}}{A_{22}}(-\kappa_{xy}) \tag{35}$$

One can further simplify eqn (35) by neglecting the term $[(\theta_0+\theta)\mathrm{D}_{66}\kappa_{xy}]/A_{12}$ of $O(\varepsilon^2)$. The result is

$$\varepsilon^0_{yy} = -\frac{A_{12}}{A_{22}}\varepsilon^0_{xx} - \frac{B_{26}}{A_{22}}(-\kappa_{xy}) \tag{36}$$

According to eqns (15) and (36), eqns (29a) and (29c) reduce to

$$\begin{Bmatrix} N_{xx} \\ M_{xy} \end{Bmatrix} = \begin{bmatrix} \alpha_{11} & \alpha_{12} \\ \alpha_{12} & \alpha_{22} \end{bmatrix} \begin{Bmatrix} \varepsilon_0 + \frac{1}{2}(\theta^2 + 2\theta_0\theta)y^2 \\ -U_{1,y} - 2\theta \end{Bmatrix} \tag{37}$$

$$Q_x = -\beta\left[U_1 + \frac{A_{12}}{A_{22}}(\theta_0+\theta)(\theta^2+2\theta_0\theta)\frac{y^3}{6} + \left\{\varepsilon_0\left(1+\frac{A_{12}}{A_{22}}\right) - 2\theta\frac{B_{26}}{A_{22}}\right\}(\theta_0+\theta)y\right] \tag{38}$$

A more accurate estimate for the out-of-plane shear stiffness coefficient, β, is derived in the Appendix by integrating equilibrium equations through the thickness.

Substitute eqns (37) and (38) into eqn (22) to obtain

$$\frac{\alpha_{22}}{\beta}U_{1,yy}-U_1=\frac{A_{12}}{A_{22}}(\theta_0+\theta)(\theta^2+2\theta_0\theta)\frac{y^3}{6}+\left[\frac{\alpha_{12}}{\beta}(\theta^2+2\theta_0\theta)+\left(1+\frac{A_{12}}{A_{22}}\right)(\theta_0+\theta)\varepsilon_0 -2\theta(\theta_0+\theta)\frac{B_{26}}{A_{22}}\right]y \quad (39)$$

Solve eqn (39) with the free edge boundary conditions

$$M_{xy}|_{y=\pm b}=0 \quad (40)$$

to get the following expression for the twisting curvature

$$\kappa_{xy}=U_{1,y}+2\theta=\frac{\cosh(sy)}{\cosh(sb)}\left[\frac{\alpha_{12}}{\alpha_{22}}\varepsilon_0-2\theta+\frac{\alpha_{12}}{\alpha_{22}}\frac{b^2}{2}(\theta^2+2\theta_0\theta)\right]+2\theta \quad (41)$$

where

$$s=\sqrt{\frac{\beta}{\alpha_{22}}} \quad (42)$$

It is worth noting that the same result for the twisting curvature in eqn (41) could be obtained by neglecting the terms of $O(\varepsilon^{3/2})$ in the strain–displacement relations (15).

Substitute eqns (41) and (37) into eqns (23) and (26), integrate, solve for ε_0 and F, to obtain the following extension-twist relationships

$$\varepsilon_0(a_4-\theta_0-\theta)=-\frac{1}{2b^3\alpha_{11}k_3}T+\left(a_1-\frac{4}{3}a_2\theta_0+2a_3\theta_0^2\right)\theta-(a_2-3a_3\theta_0)\theta^2+a_3\theta^3$$

$$F(a_4-\theta_0-\theta)=-\frac{k_4}{b^2}T+\left(b_1-\frac{4}{3}b_2\theta_0+2b_3\theta_0^2\right)\theta-(b_2-3b_3\theta_1)\theta^2+b_3\theta^3 \quad (43)$$

where the constants a_i and b_i are defined as

$$a_1=\frac{4\alpha_{22}}{b^2\alpha_{11}}\frac{k_1}{k_3}$$

$$a_2=-\frac{3\alpha_{12}}{\alpha_{11}}\frac{k_2}{k_3}$$

$$a_3=\frac{b^2}{2k_3}\left(k_3-\frac{2}{15}\right)$$

$$a_4=\frac{2\alpha_{12}}{b^2\alpha_{11}}\frac{k_1}{k_3}$$

$$b_1=\frac{8\psi}{ba_{11}}\frac{k_1}{k_3}$$

$$b_2 = -6b\alpha_{12}[k_1 + k_2 k_4]$$
$$b_3 = b^3\alpha_{11}\left[-k_3 + k_4\left(k_3 - \frac{2}{15}\right)\right] \tag{44}$$

and

$$k_1 = 1 - \frac{\tanh(bs)}{bs}$$
$$k_2 = \frac{2}{3} - k_1$$
$$k_3 = \frac{1}{3} - \frac{\alpha_{12}^2}{\alpha_{11}\alpha_{22}}(1 - k_1)$$
$$k_4 = \frac{\psi + \alpha_{12}^2 k_1}{\alpha_{11}\alpha_{22}k_3}$$
$$\psi = \alpha_{11}\alpha_{22} - \alpha_{12}^2 \tag{45}$$

The same extension-twist relationships (43) could be obtained if the terms of $O(\varepsilon^{3/2})$ were neglected in the strain–displacement relations.

It is useful to obtain a solution based on the classical shell theory assumptions and compare the resulting extension-twist relations with eqns (43). According to the Kirchhoff–Love assumptions a straight line element normal to the middle surface in the initial state remains normal to the deformed middle surface and does not change in length. For small strains this assumption is expressed by

$$\varepsilon_{zz} = \gamma_{yz} = \gamma_{xz} = 0 \tag{46}$$

After substituting eqns (46) into eqns (15), and neglecting the terms of $O(\varepsilon)$ compared to one, the twisting curvature expression reduces to

$$\kappa_{xy} = U_{1,y} + 2\theta \cong 2\theta \tag{47}$$

which corresponds to the Saint Vénant type warping for a thin strip. Note that eqn (47) can be obtained neglecting the exponential term in eqn (41). That is, for a thin strip the out-of-plane strain contribution is associated with the free edge effect only. Substitute eqns (47) and (37) into eqns (23) and (26) to obtain eqns (43) with constants a_i and b_i taking the following form

$$a_1 = \frac{12\alpha_{22}}{b^2\alpha_{11}}, \quad a_2 = \frac{3\alpha_{12}}{\alpha_{11}}, \quad a_3 = 0.3b^2, \quad a_4 = \frac{6\alpha_{12}}{b^2\alpha_{11}}$$
$$b_1 = \frac{24\psi}{b\alpha_{11}}, \quad b_2 = 0, \quad b_3 = \frac{4b^3\alpha_{11}}{15}$$
$$k_3 = \frac{1}{3}, \quad k_4 = 3 \tag{48}$$

Equations (48) can also be obtained directly from eqns (44) and (45) by neglecting the term $1/(bs)$ compared to unity. According to eqns (42) and (32), this is equivalent to eliminating the contribution of the transverse shear stiffness to the extension-twist relations. Note that a material satisfying eqns (46) can be considered as out-of-plane rigid since out-of-plane stresses are generally not zero.

It is worth noting that the extension-twist relationships (43) with the coefficients given by eqns (48), which represent the out-of-plane rigid strip solution, can also be obtained from the geometrically nonlinear analysis of Hodges et al. (1996). In this analysis, based on an asymptotical formulation, contribution of the out-of-plane shear is neglected as in the classical laminated plate theory.

Finally, the following linear extension-twist relations can be derived from eqns (43)

$$\begin{Bmatrix} \varepsilon_0 \\ \theta \end{Bmatrix} = \begin{bmatrix} s_{11} & s_{12} \\ s_{12} & s_{22} \end{bmatrix} \begin{Bmatrix} F \\ T \end{Bmatrix} \tag{49}$$

where the compliances, expressed as

$$s_{11} = \frac{a_1 - \frac{4}{3}a_2\theta_0 + 2a_3\theta_0^2}{b_1 - \frac{4}{3}b_2\theta_0 + 2b_3\theta_0^2}, \quad s_{12} = \frac{a_4 - \theta_0}{b_1 - \frac{4}{3}b_2\theta_0 + 2b_3\theta_0^2}, \quad s_{22} = \frac{k_4}{b^2}\frac{1}{b_1 - \frac{4}{3}b_2\theta_0 + 2b_3\theta_0^2} \tag{50}$$

account for a finite pretwist. A comparison between eqns (49) and (50), and other analytical work is provided in the Application section.

3. Application

The axial force-twist relationship (43) is compared with test data for strips made of ICI Fiberite T300/954-3 Graphite/Cyanate material system with properties given in Table 1. Two stacking sequences, $[20_2/-70_4/20_2/-20_2/70_4/-20_2]_T$ and $[30_2/-60_4/30_2/\ -30_2/60_4/-30_2]_T$, are used. The length, the width and the thickness of the laminates are 254, 25.4 and 1.168 mm, respectively. The strips have an end pretwist angle of 5°. Four specimens of each stacking sequence were tested. Their manufacturing and testing details are described in Armanios et al. (1996). The results are presented in Figs 4 and 5 where the absolute values of the end twist angle, θL, are plotted as a function of the axial force. The test data are labeled specimens 1–4 in the figures, and the predictions of eqn (49) (Linear model) are included for comparison.

It is worth noting that the full solution, where the coefficients are given by eqns (44) and (45), and the out-of-plane rigid strip solution, where the coefficients are defined in eqns (48), are within 1% relative difference in predictions of the axial force-twist relationship for both stacking sequences.

Further verification of the accuracy of the closed-form solution is provided by a geometrically nonlinear finite element simulation. The strips were modeled by 800 quadrilateral shell elements, S4R, in the ABAQUS code. The total number of degrees of freedom was 5346. The results are labeled as ABAQUS in Figs 4 and 5. The predictions of eqn (43) are in excellent agreement with the test data and with the finite element solution.

In addition to the comparison made between the extension-twist relations (43) and analysis of

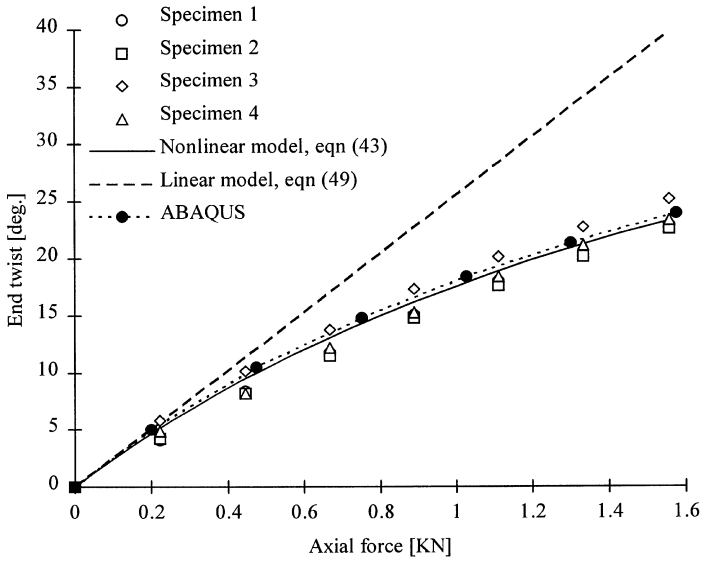

Fig. 4. Comparison of model predictions with test data for a $[20_2/-70_4/20_2/-20_2/70_4/-20_2]_T$ strip.

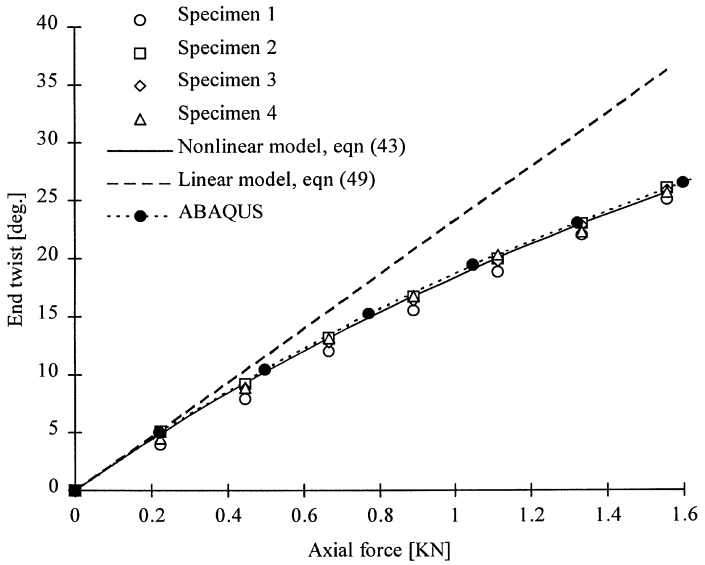

Fig. 5. Comparison of model predictions with test data for a $[30_2/-60_4/30_2/-30_2/60_4/-30_2]_T$ strip.

Hodges et al. (1996), the predictions of the present analysis are compared to the results from the linear model of Kosmatka (1991) for pretwisted laminates. This model is the Ritz method based and applied to the analysis of extension-twist coupling behavior for antisymmetric $[\alpha/-\alpha]_T$ angle-ply laminates with an arbitrarily large pretwist.

Table 2
Properties of T300/5208 Graphite/Epoxy material system (Kosmatka, 1991)

$E_{11} = 132.2$ GPa
$E_{22} = E_{33} = 10.75$ GPa
$G_{12} = G_{13} = G_{23} = 5.65$ GPa
$v_{12} = v_{13} = 0.239$
$v_{23} = 0.4$

One can extract the following linear axial strain-twist relationship (no applied torque) from eqns (49) and (50)

$$\theta = c\varepsilon_0 \tag{51}$$

where

$$c = \frac{a_4 - \theta_0}{a_1 - \frac{4}{3}a_2\theta_0 + 2a_3\theta_0^2} \tag{52}$$

Equation (52) is compared with the solution of Kosmatka (1991) for T300/5208 Graphite/Epoxy material system with properties provided in Table 2. The laminate thickness is 10% of its width and the stacking sequence is $[-\alpha/\alpha]_T$. The plots of the twist-extension ratio defined as

$$\xi_0 = 2bc \tag{53}$$

vs the ply angle α for different values of the pretwist parameter defined as

$$p = 2b\theta_0 \tag{54}$$

are shown in Fig. 6. The case of $p = 0$ corresponds to the classical lamination theory prediction and is included for illustrating the trend in the twist-extension ratio variation with the ply angle. The predictions of eqn (52), labeled as closed-form in Fig. 6, are in excellent agreement with the numerical solution.

Next, the compliances defined in eqns (50) are compared with the solution of Kosmatka (1991). Denote

$$s_{11}^0 = s_{11}|_{\alpha=p=0}, \quad s_{22}^0 = s_{22}|_{\alpha=p=0} \tag{55}$$

The plots of

$$\frac{s_{11}^0}{s_{11}}, \quad s_{12}E_{11}(2b)^3, \quad \frac{s_{22}^0}{s_{22}} \tag{56}$$

as functions of α for different values of p are presented in Figs 7–9. The case of $p = 0$ is included in the figures for trend illustration. The closed-form and the numerical solutions are in excellent agreement for s_{11}^0/s_{11} and $s_{12}E_{11}(2b)^3$. The comparison in Fig. 9 indicates good agreement for s_{22}^0/s_{22} at $p = 0.1$ and 0.2. However, a maximum discrepancy of 19% exists at $p = 0.3$ and $\alpha = 0$.

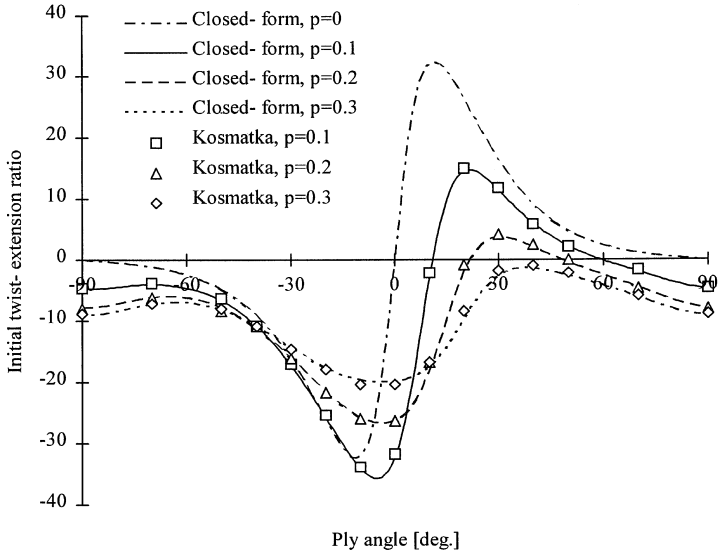

Fig. 6. Comparison of closed-form and numerical solutions.

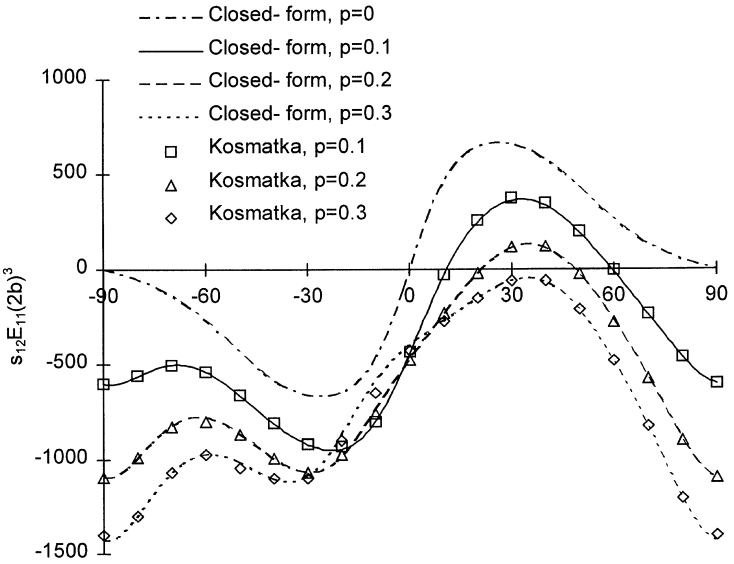

Fig. 7. Comparison of closed-form and numerical solutions.

A similar discrepancy in the torsional rigidity predictions at $p = 0.3$ and small ply angles is found between the closed-form solution and the finite element solution of Cesnik and Hodges (1997). An investigation into this discrepancy is provided in the following.

In the case of $\alpha = 0$, corresponding to the unidirectional orthotropic strip, the following expression for s_{22}^0/s_{22} can be obtained from eqns (50)

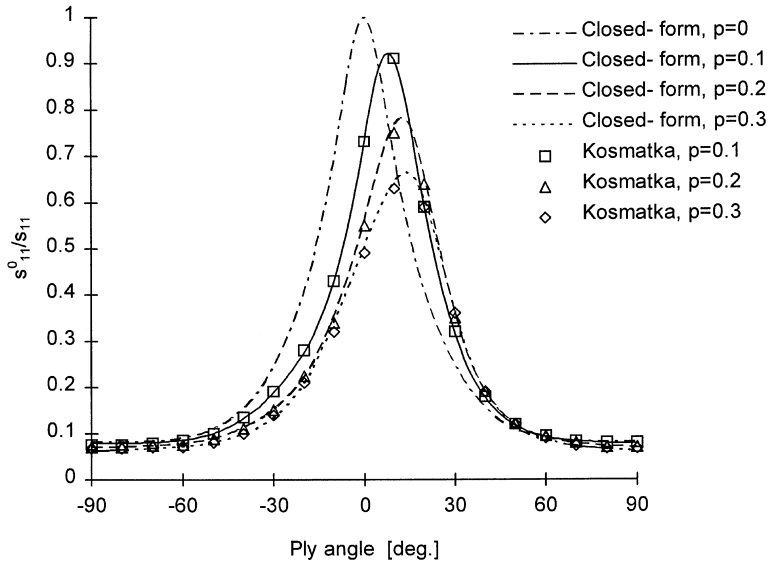

Fig. 8. Comparison of closed-form and numerical solutions.

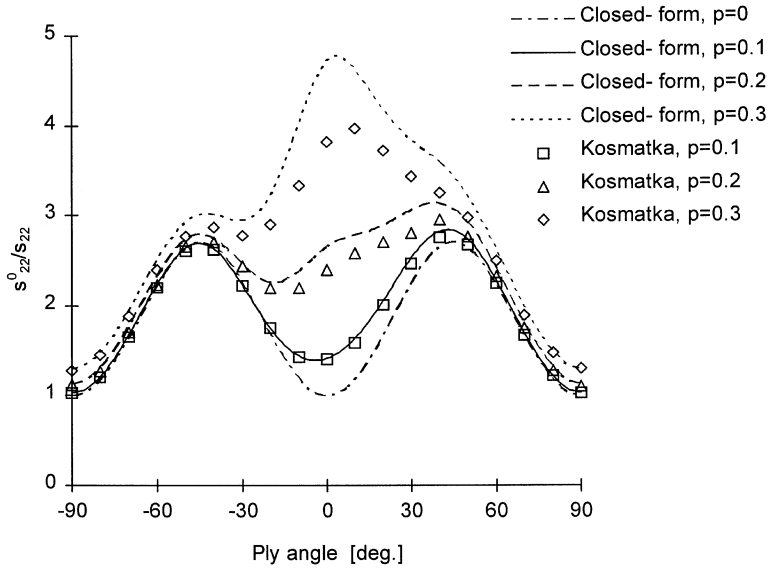

Fig. 9. Comparison of closed-form and numerical solutions.

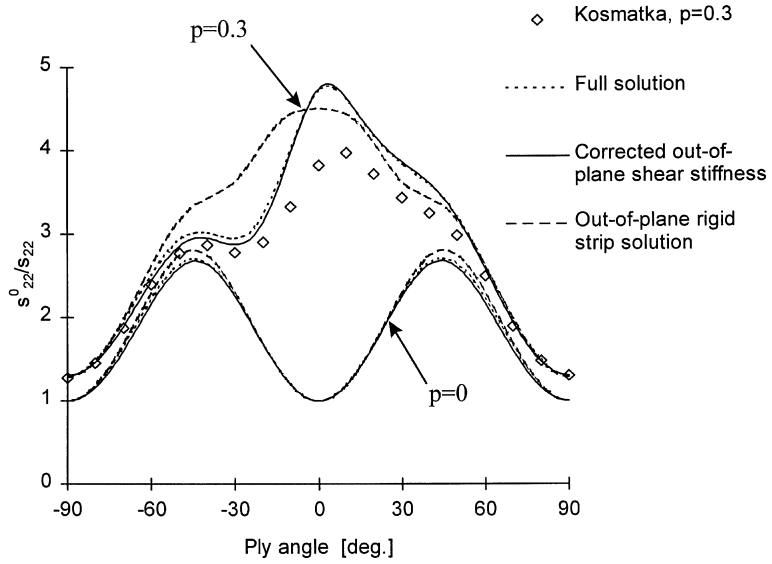

Fig. 10. Comparison of torsional rigidity predictions.

$$\frac{s^0_{22}}{s_{22}} = 1 + \left(\frac{E_{11}}{G_{12}}\right)\frac{1}{15k_1}\left(\frac{b}{h}\right)^2 p^2 \tag{57}$$

where

$$k_1 = 1 - \frac{\tanh(bs)}{bs}, \quad bs = 2\sqrt{\frac{3G_{13}}{G_{12}}}\left(\frac{b}{h}\right) \tag{58}$$

Equation (57) indicates that the torsional rigidity ratio is influenced by the E_{11}/G_{12} ratio, the out-of-plane shear stiffness, and the geometry. Setting $k_1 = 1$ in eqn (57) is equivalent to neglecting the contribution of the out-of-plane shear strains. The associated error is 5% at $p = 0.3$.

It is worth noting that the maximum pretwist considered, $p = 0.3$, corresponds to strips with 172° per 10 in (172° per 254 mm). For such a pretwist, neglecting the quantity $(\theta_0 b)^2$ compared to one causes an acceptable error of 2%. However, the ratio $(h/b) = 0.2$ is at the limit of the thin strip assumption; hence, the out-of-plane shear effect could be significant. Indeed, the term $[1/(bs)] = O(h/b)$ was neglected compared to one in deriving eqns (48) which represent the out-of-plane rigid strip solution. A model for correcting the out-of-plane shear stiffness is presented in the Appendix. A comparison of the influence of this correction on the s^0_{22}/s_{22} ratio prediction is provided in Fig. 10 for flat strips ($p = 0$) and for strips with $p = 0.3$. The full solution model in the figure corresponds to the coefficients defined in eqns (44) and (45). The corrected out-of-plane shear stiffness is based on eqn (A9) while the out-of-plane rigid strip solution uses the coefficients in eqns (48). All models show the same trends for the flat strips, but in the highly pretwisted case neglecting the out-of-plane shear strains gives 27% maximum error relative to the full solution. For the material system provided in Table 2, the correction to the out-of-plane shear stiffness does

not result in considerable difference for the torsional rigidity predictions compared to the full solution, since the lamina out-of-plane shear moduli, G_{23} and G_{13}, are equal. The discrepancy would be larger for laminates with highly nonhomogeneous shear stiffnesses of plies.

4. Conclusion

A finite displacement model for pretwisted laminated composite strips with extension-twist coupling is presented. It is shown that consistent with the small strain assumption, the effect of the terms of $O(\varepsilon^{3/2})$ in the strain–displacement relations on the results is negligible for typical laminates. The accuracy of the closed-form extension-twist relationships is assessed through comparison with test data and with predictions from existing models. It is found that the influence of out-of-plane shear strains can become significant as the thickness-to-width ratio approaches the limit of the thin strip assumption.

Acknowledgements

This work is sponsored by the National Rotorcraft Technology Center under Grant NCC2-945. This support is gratefully acknowledged.

Appendix. Out-of-plane shear stiffness (small displacements)

According to the equilibrium equations

$$\sigma_{xy,y}+\sigma_{xz,z}=0, \quad \sigma_{yy,y}+\sigma_{yz,z}=0 \tag{A1}$$

and the traction free boundary conditions, the out-of-plane shear stresses can be expressed as follows

$$\sigma_{xz}=-\int_{-(h/2)}^{z}\sigma_{xy,y}\,\mathrm{d}z, \quad \sigma_{yz}=-\int_{-(h/2)}^{z}\sigma_{yy,y}\,\mathrm{d}z \tag{A2}$$

The necessary in-plane constitutive relations for a lamina are

$$\begin{aligned}\sigma_{yy}&=\bar{Q}_{12}\varepsilon_{xx}+\bar{Q}_{22}\varepsilon_{yy}+\bar{Q}_{26}\gamma_{xy}\\ \sigma_{xy}&=\bar{Q}_{16}\varepsilon_{xx}+\bar{Q}_{26}\varepsilon_{yy}+\bar{Q}_{66}\gamma_{xy}\end{aligned} \tag{A3}$$

where $\bar{Q}_{ij}$ are components of the lamina stiffness matrix.

For small displacements the expression for the longitudinal strain changes from eqn (15) to

$$\varepsilon_{xx}=\varepsilon^{0}_{xx}-z\kappa_{xx}=\varepsilon_{0} \tag{A4}$$

and eqn (21) reduces to

$$N_{yy}=0 \tag{A5}$$

Substitute eqns (20), (A4) and (A5) into eqns (29) to obtain

$$\varepsilon_{yy} = \varepsilon^0_{yy} = -\left(\frac{A_{12}D_{66} - B_{16}B_{26}}{A_{22}D_{66} - B^2_{26}}\right)\varepsilon_0 - \left(\frac{B_{26}}{A_{22}D_{66} - B^2_{26}}\right)M_{xy}$$

$$\gamma_{xy} = -z\kappa_{xy} = -z\left(\frac{A_{22}B_{16} - A_{12}B_{26}}{A_{22}D_{66} - B^2_{26}}\right)\varepsilon_0 + z\left(\frac{A_{22}}{A_{22}D_{66} - B^2_{26}}\right)M_{xy} \tag{A6}$$

Substitute eqns (A3), (A4), (A6) into eqns (A2), and use the equilibrium eqn (22) to obtain the following out-of-plane shear stress distribution

$$\sigma_{xz} = \frac{Q_x}{A_{22}D_{66} - B^2_{26}}\int_{-(h/2)}^{z}(\bar{Q}_{26}B_{26} - z\bar{Q}_{66}A_{22})\,\mathrm{d}z$$

$$\sigma_{yz} = \frac{Q_x}{A_{22}D_{66} - B^2_{26}}\int_{-(h/2)}^{z}(\bar{Q}_{22}B_{26} - z\bar{Q}_{26}A_{22})\,\mathrm{d}z \tag{A7}$$

Note that $\sigma_{yz} = \sigma_{xz} = 0$ on the lower and the upper surfaces of the laminate.

The complementary energy due to the out-of-plane shear can be expressed as

$$U^c = \frac{L}{2}\int_{-b}^{b}\frac{Q^2_x}{\beta^*}\mathrm{d}y = \frac{L}{2}\int_{-b}^{b}\mathrm{d}y\int_{-(h/2)}^{h/2}(\bar{S}_{44}\sigma^2_{yz} + 2\bar{S}_{45}\sigma_{yz}\sigma_{xz} + \bar{S}_{55}\sigma^2_{xz})\,\mathrm{d}z \tag{A8}$$

where β^* is the out-of-plane shear stiffness coefficient, and $\bar{S}_{44}$, $\bar{S}_{45}$, $\bar{S}_{55}$ are components of the lamina compliance matrix. Substitute eqns (A7) into eqn (A8) to obtain

$$\frac{1}{\beta^*} = \frac{1}{(A_{22}D_{66} - B^2_{26})^2}\int_{-(h/2)}^{h/2}(\bar{S}_{44}\bar{\sigma}^2_{yz} + 2\bar{S}_{45}\bar{\sigma}_{yz}\bar{\sigma}_{xz} + \bar{S}_{55}\bar{\sigma}^2_{xz})\,\mathrm{d}z \tag{A9}$$

where

$$\bar{\sigma}_{yz} = \int_{-(h/2)}^{z}(\bar{Q}_{22}B_{26} - z\bar{Q}_{26}A_{22})\,\mathrm{d}z, \quad \bar{\sigma}_{xz} = \int_{-(h/2)}^{z}(\bar{Q}_{26}B_{26} - z\bar{Q}_{66}A_{22})\,\mathrm{d}z \tag{A10}$$

References

Armanios, E. A., Makeev, A. and Hooke, D. A. (1996) Finite displacement analysis of laminated composite strips with extension-twist coupling. *Journal of Aerospace Engineering*, *ASCE* **9**(3), 80–91.

Cesnik, C. E. S. and Hodges, D. H. (1997) VABS: A new concept for composite rotor blade modeling. *Journal of the American Helicopter Society* **42**(1), 27–38.

Hodges, D. H., Harursampath, D. and Cesnik, C. E. S. (1996) Nonlinear strain field effects in anisotropic strips. *Proceedings of Recent Developments in Solid Mechanics*, Rio de Janeiro, Brazil, pp. 71–78.

Kosmatka, J. B. (1991) Extension-bend-twist coupling behavior of thin-walled advanced composite beams with initial twist. *Proceedings of the* 32*nd Structures*, *Structural Dynamics and Materials Conference*. Baltimore, Maryland, pp. 1037–1049, AIAA Paper 91-1023.

Vinson, J. R. and Sierakowski, R. L. (1986) *The Behavior of Structures Composed of Composite Materials*. Martinus Nijhoff Publishers.